Laser-Induced Potential Transients on a Au(111) Single-Crystal Electrode. Determination of the Potential of Maximum Entropy of Double-Layer Formation

Víctor Climent, Barry A. Coles, and Richard G. Compton*

Physical and Theoretical Chemistry Laboratory, Oxford University, South Parks Road, Oxford OX1 3QZ, United Kingdom

Received: January 10, 2002

Illumination of the surface of a Au(111) single-crystal electrode with short pulses of high-power laser light has been used to produce a sudden increase of its temperature. From the evolution of the open circuit potential during the temperature relaxation after the laser pulse, it is possible to obtain a relative measurement of the entropy of formation of the double layer. The electrode potential, where the potential transient is zero, has been identified with the potential of maximum entropy of formation of the double layer. This methodology has been applied to study the double layer formed between the Au(111) electrode and perchloric and sulfuric acid solutions. In both cases, it has been found that the potential of maximum entropy is located slightly negative to the potential of zero charge, corresponding to a negative contribution of the water-dipole moments to the electrode−solution potential drop. In addition, in the case of sulfuric acid solutions, a sharp increase of the relaxation time after the temperature change has been observed at potentials just below the phase transition to form the ($\sqrt{3}$x$\sqrt{7}$) adlayer. This has been explained in terms of formation of sulfate islands of reduced mobility in this potential region.

1. Introduction

The introduction of new techniques for the preparation of single-crystal surfaces has enabled an important increase of our knowledge of the electrochemistry of solid electrodes. In particular, the introduction of the flame annealing treatment for decontamination and reordering of the metallic surface as an alternative to the more expensive methods, based on ultrahigh vacuum technology, represents a key moment of the development of Interfacial Electrochemistry as a Surface Science.[1−3] However, despite this important breakthrough, the application of thermodynamic analysis to solid electrodes has not yet achieved the degree of development obtained in the past for liquid metals. This is especially true when we consider the relatively small number of experiments in which the temperature is varied as an additional thermodynamic variable.

A thermodynamic study involving variation of the temperature can provide valuable information. The entropy of formation of the interface can be obtained from the temperature coefficients of the electrode potential.[4−7] However, little work has been done in this direction with solid electrodes.[8−13]

The illumination of a metallic electrode surface with a high power laser source suddenly increases the temperature of the interfacial region. This effect constituted the base of the so-called temperature jump method. This method was developed in the eighties by Benderskii et al.[14,15] and applied to the study of the electrochemical double layer between an aqueous solution and a mercury electrode. From a proper analysis of the temperature coefficient of the potential drop at the metal|solution interface extracted from these experiments, it is possible to extract the entropy of formation of the double layer. A similar approach was used by Feldberg et al.,[16−18] but the method was applied to investigate kinetics of electrochemical processes. Also, from a potentiostatic heating of the electrode surface with the laser light we have shown that it is possible to identify the sign of the double-layer charge, and consequently, the location of the potential of zero charge.[19]

It is assumed that the only effect of the laser is the heating of the electrode surface, resulting in a sudden temperature change of the interface. Due to the relatively high power introduced in the system, the temperature change takes place in a very short time scale, allowing the study of fast processes. However, to apply a thermodynamic analysis, the rate of the temperature change should be slower than the time needed to reach an equilibrium state (relaxation time). Otherwise, the kinetics of the processes involved need to be considered.

In the present work, we have applied the temperature jump method to extract thermodynamic information about the electrochemical double layer between a Au(111) single-crystal electrode and perchloric or sulfuric acid solutions. The most significant parameter that can be extracted from this method is the potential where the entropy of formation of the interface is maximum, which has been found to be located at potentials slightly negative with respect of the potential of zero charge (pzc). The paper is structured as follow: first, theoretical considerations about the time dependence of the temperature change and its influence on interfacial properties are developed. Then, the response of the double-layer potential to the sudden change of the temperature is studied for perchloric and sulfuric acid solutions. To check the influence of the thermodiffusion potential on the potential change measured, some experiments were also performed on slightly acidified potassium perchlorate and sulfate solutions.

2. Preliminary Considerations

2.1. Laser Heating. The temperature change after a laser pulse, considering negligible penetration depth of the light (i.e., all the nonreflected part of the radiation is instantaneously

* To whom all correspondence should be addressed. Email: compton@ermine.ox.ac.uk, Tel.: +44 (0) 1865 275 413, FAX: +44 (0) 1865 275 410.

10.1021/jp020054q CCC: $22.00
Published on Web 05/01/2002

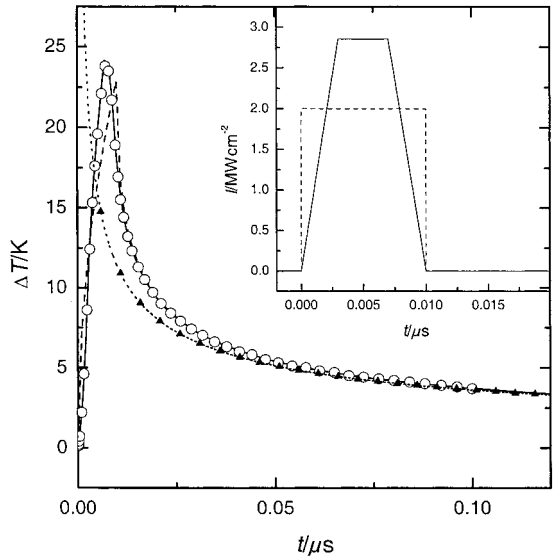

Figure 1. Theoretical temperature change produced by a laser pulse of 20 mJ cm^{-2} on a gold substrate. Lines: Negligible penetration depth, nonuniform (solid line) and uniform (dashed line) temporal pulse shape; Circles: Finite penetration depth and nonuniform temporal pulse shape. Dotted line with triangles: Approximate temperature decay proportional with the reciprocal of $\sqrt{t}$. Inset: Temporal pulse shapes used in the calculation.

converted into heat at the surface of the electrode), is given by the following expression:[14]

$$\Delta T(t) = \frac{1}{\sqrt{\pi\kappa c d} + \sqrt{\pi\kappa_1 c_1 d_1}} \int_0^t q(t-t') \frac{1}{\sqrt{t'}} \mathrm{d}t' \qquad (1)$$

where κ, c, and d and κ_1, c_1, and d_1 are the thermal conductivity, thermal capacity, and density of gold and the aqueous solution, respectively. q is the power density adsorbed by the metal, which depends on the temporal shape of the laser pulse:

$$q(t) = (1-R)I(t)$$

where R is the reflectivity of the surface and $I(t)$ is the time-dependent energy flux per unit of area.

For a uniform laser pulse the integration on eq 1 can be evaluated easily, resulting in the following:

$$\Delta T(t) = \frac{2(1-R)I}{\sqrt{\pi\kappa c d} + \sqrt{\pi\kappa_1 c_1 d_1}} \sqrt{t} \quad t \le t_0 \text{ Heating} \qquad (2)$$

$$\Delta T(t) = \frac{2(1-R)I}{\sqrt{\pi\kappa c d} + \sqrt{\pi\kappa_1 c_1 d_1}} [\sqrt{t} - \sqrt{t-t_0}] \quad t > t_0 \text{ Cooling} \qquad (3)$$

For long times, it is possible to expand the $\sqrt{t-t_0}$ term, keeping only the lower terms in the series. According to this approximation the temperature falls with time as:

$$\Delta T(t) = \frac{1}{2}\Delta T_0 \sqrt{\frac{t_0}{t}} \qquad (4)$$

Figure 1 shows the temperature change evaluated with expression (1) for a uniform (equations (2) and (3)) and a particular nonuniform laser shape (as indicated in the inset). Also plotted in the same figure is the temperature change obtained with a finite element simulation (using FIDAP, Fluent Inc., http://www.fluent.com), taking into account the finite penetration depth of the light into the gold substrate (penetration depth is ca. 20 nm[20,21]) and the same nonuniform laser shape. The agreement between the penetrating and nonpenetrating calculation is excellent, supporting the use of eq 1. Another observation from Figure 1 is that the effect of the different pulse shapes is only noticeable at times shorter than 0.02 μs. Figure 1 also includes the approximate temperature decay given by eq 4. It can be seen that after ca. 0.1 μs the different functions become indistinguishable and the use of the simplified expression (4) is fully justified.

TABLE 1: Some Ionic Entropies of Transport:[22]

Ion	S/J mol^{-1} K^{-1}	ion	S/J mol^{-1} K^{-1}
H^+	39.44[a]	SO_4^{2-}	26.96[b]
K^+	4.40[a]	ClO_4^-	−3.10[c]

[a] Calculated from conventional heats of transport in 0.05 m aqueous solutions at 25° C. [b] Calculated from conventional heats of transport at infinite dilution and 25° C. [c] Calculated from conventional heats of transport in 0.01 m aqueous solutions at 25° C.

2.2. Thermodynamic Implications. According to expression (4), and if the temperature change is small enough to allow a linear variation of the potential with the temperature, we can write:

$$\Delta E = \left(\frac{\partial E}{\partial T}\right)_q \Delta T = \left(\frac{\partial E}{\partial T}\right)_q \frac{1}{2}\Delta T_0 \sqrt{\frac{t_0}{t}} \qquad (5)$$

Then, the temperature coefficient of the open circuit potential can be extracted from the slope of the plot of ΔE vs $1/\sqrt{t}$. Moreover, from the electrocapillary equation it is possible to show:[5,7]

$$\left(\frac{\partial E}{\partial T}\right)_q = -\left(\frac{\partial \Delta S}{\partial q}\right)_T \qquad (6)$$

where ΔS is the interfacial entropy of formation of the interface. Hence, by integrating a plot of the slopes of the ΔE vs $1/\sqrt{t}$ as a function of the double-layer charge it is possible to obtain a plot of ΔS. Note that when the curve ΔS vs q passes through a maximum, $(\partial \Delta S/\partial q)_T$ will be zero, and so will be the potential change due to the electrode heating. Hence, the potential of zero transient (pzt) can be identified with the potential of maximum entropy of double layer formation.

One possible limitation with the above analysis is the existence of a thermodiffusion potential contributing to the open circuit potential measured after heating the electrode with the laser pulse. However, thermodiffusion potentials can be estimated from a knowledge of the entropy of transport (or Eastman entropy of transfer) of the involved ions, according to the expression:[22]

$$\frac{\Delta E_{\text{Thermodiffusion}}}{\Delta T} = -\frac{1}{F}\sum \frac{t_i}{z_i}\hat{S}_i \qquad (7)$$

where t_i, z_i, and $\hat{S}_i$ are the transport number, the charge (with its sign) and the Eastman entropy of transport of the ion i, respectively. Some values of these properties, corresponding to the ions composing the solutions employed in this study, are given in Tables 1 and 2. As deduced from them, the thermodiffusion potential is more important in acid solutions due to the abnormally large entropy of transport of the proton. Hence, another way of checking the influence of this phenomenon on the measured potential transients is to compare results at different pHs, the thermodiffusion effect being expected to be negligible for neutral solutions. It is worth pointing out, that

TABLE 2: Transport Numbers for the Solutions Used in This Study

solution	t_{H+}	t_{K+}
0.1 M $HClO_4$	0.849[a]	
0.1 M H2SO_4	0.819[a]	
0.1 M K_2SO_4+1 mM H_2SO_4	0.022[b]	0.466[b]

[a] From Breck et al.[32] [b] Calculated from the mobilities of the ions in infinitely diluted solutions.

this potential contribution should be independent of the electrode potential, and depend only on the nature of the electrolytic solution.

Equation 5 is only valid if the reestablishment of the potential drop at the double layer after the temperature variation takes place instantaneously. However, if we consider a first-order kinetic for this relaxation it is possible to write:

$$\frac{d\Delta E}{dt} = -k[\Delta E - \xi \Delta T] \tag{8}$$

where $\xi = (\partial \Delta E/\partial T)_q$. Applying Laplace transform techniques, it is possible to show that, in this case, the potential transient is given by:

$$\Delta E = \frac{\xi}{\tau}\int_0^t \Delta T(t') e^{-(t-t')/\tau}\, dt' \tag{9}$$

If we take into account the existence of a thermodiffusion potential, a second term should be added to eq 9. The establishment of a thermodiffusion potential is very fast, as compared with the time scale of the present experiments.[23,24] Then, eq 9 can be rewritten:

$$\Delta E(t) = \frac{\xi_1}{\tau}\int_0^t \Delta T(t') e^{(t-t')/\tau}\, dt' + \xi_2 \Delta T(t) \tag{10}$$

where ξ_2 is temperature coefficient for the thermodiffusion potential. The fitting of the experimental values to eq 10 is not straightforward, since it implies a numerical integration. However, the analysis can be simplified by doing the fitting in the Laplace space. Taking Laplace transforms on both sides of eq 10 a simpler equation is obtained:

$$\frac{\overline{\Delta E}}{\overline{\Delta T}} = \frac{\xi_1}{\tau}\frac{1}{s + \tau^{-1}} + \xi_2 \tag{11}$$

where $\overline{\Delta E}$ and $\overline{\Delta T}$ stand for the Laplace transform of the experimental potential transients and the temperature change, respectively. Using equation (3), $\overline{\Delta T}$ can be calculated:

$$\overline{\Delta T} = A\frac{\sqrt{\pi}}{2s^{3/2}}(1 - e^{-t_0 s}) \tag{12}$$

where s is the Laplace variable and $(A = 2(1 - R)I)/(\sqrt{\pi \kappa c d} + \sqrt{\pi \kappa_1 c_1 d_1}$. $\overline{\Delta E}$ can be calculated from the experimental values, evaluating numerically the integral:

$$\overline{\Delta E} = \int_0^{t_f} \Delta E(t) e^{-st}\, dt \tag{13}$$

where t_f is the longest time until which the potential transient has been monitored. Since $\Delta E(t)$ is decreasing after t_f, the error due to the truncation of experimental values after t_f will be smaller than $\Delta E(t_f)/s\, e^{-stf}$. The resulting values of $\overline{\Delta E}/\overline{\Delta T}$ can then be easily fitted to eq 11 by standard procedures. Moreover, if we introduce the time constant of the operational amplifier (40 MHz), eq 11 is transformed into:

$$\frac{\overline{\Delta E}}{\overline{\Delta T}} = \frac{\xi_1}{\tau}\frac{1}{s + \tau^{-1}} + \frac{\xi_2}{\tau_2}\frac{1}{s + \tau_2^{-1}} \tag{14}$$

where τ_2 can be taken as ca. 1/40 μs.

3. Experimental Section

The light source employed was a GCR 130 Q-switched Nd:YAG laser (Spectra Physics Lasers, Inc., CA) operating in frequency doubled mode at a wavelength of 532 nm and pulse duration of 10 ns. The beam diameter obtained directly at the laser output is ca. 7 mm and this was reduced to ca. 3.5 mm by passing it through a conventional arrangement of lenses. The energy of each single pulse was set to 1−5 mJ (ca. 8−50 mJ cm^{-2}). With the use of eq 2, a maximum temperature change of 10−60 K is expected, respectively. Optics housings and lenses were supplied by Newport Corporation and mirrors obtained from Comar Instruments (Cambridge, UK). The laser power was determined with a Gentec ED-200L detector head in conjunction with a Gentec SUN Series EM-1 Energy Meter (Gentec, CA).

Experiments were performed in a conventional three-electrode arrangement. The Au(111) single-crystal electrode was prepared at the University of Alicante from a small gold bead (2 mm), oriented, cut, and polished to obtain the Au(111) orientation, following Clavilier's procedure.[25] Prior to each experiment, the electrode was flame annealed in a butane + air flame, cooled in the atmosphere of the laboratory, and then protected with a drop of ultrapure water. A platinum mesh (Goodfellow Cambridge Ltd., Cambridge, UK) was used as a counter electrode and a Pd wire charged with H_2 in a separate compartment was used as a reference electrode. However, all potentials are quoted against the SCE reference electrode through this paper. To make the conversion, the potential difference between a SCE reference electrode and the Pd/H_2 electrode was directly measured at the end of each experimental session.

A computer-controlled μ-Autolab potentiostat (Eco-Chemie, Utrecht, Netherlands) was employed to control the potential applied at the working electrode during the control voltammetric experiments. However, for recording the potential transients after the laser firing, a potentiostat of in-house design was employed. The experimental protocol is as follows: after recording a voltammogram to ensure the surface order and cleanliness of the solution, the electrode is polarized at a given potential. Around 200 μs before firing the laser, the counter electrode is disconnected, with a relay (BT55, release time 25 μs, bounce time 100 μs) leaving the working electrode at open circuit potential. The potential of the reference electrode is measured with respect to the working electrode (which is grounded), while the laser is fired on the surface, producing the rise of the temperature. The operational amplifier used to follow the potential of the reference is a AD825, with a bandwidth of 41 MHz. From equations (3) and (4) it can be deduced that after several μs the temperature has essentially returned to the ambient value. This allows repetition of the experiment in order to average multiple transients. The experiment was repeated at a frequency of 10 Hz, which allows the attainment of the equilibrium temperature between consecutive pulses. The counter electrode is reconnected 3 ms after the laser pulse and disconnected again ca. 200 μs before the following pulse, ensuring that the potential is kept at the desired value, and avoiding any drift of the electrode potential while the circuit is

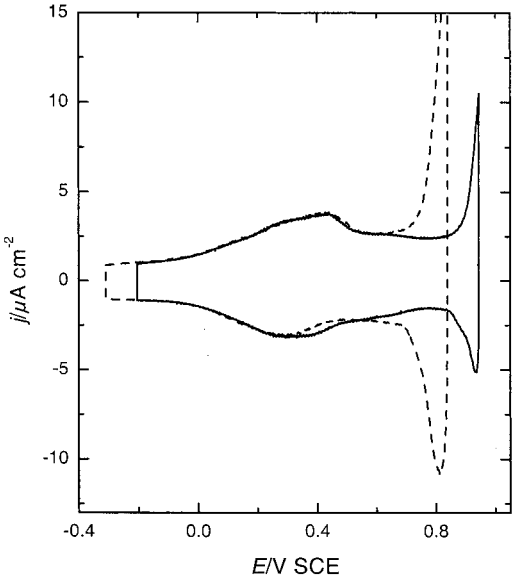

Figure 2. Cyclic voltammograms corresponding to a Au(111) single-crystal electrode in 0.1 M $HClO_4$ (solid line) and 0.1 M $KClO_4$ + 1 mM $HClO_4$ (dashed line) solutions. Sweep rate: 50 mV s^{-1}.

open. At each potential, 256 potential transients were averaged using a TDS 3032 Tektronix oscilloscope.

To ensure that the potential transient actually corresponds to a process caused by the illumination of the electrode and that it is not a mere artifact, the experiment is repeated with the beam intercepted from impinging on the electrode. The potential transient disappears when this is done, and only oscillating noise is recorded in this case. The transient recorded with the beam intercepted is subtracted as a baseline from each potential transient and the results shown below corresponds to the result after this correction.

The charges needed for the integration of eq 6 were obtained from chronocoulometric experiments in which the potential was stepped from consecutively higher potentials to 0.05 V (vs Pd/H_2). The potential of zero charge was obtained from the minimum of the differential capacity for diluted perchloric acid solutions and extrapolated for the 0.1 M concentration.

Solutions were prepared from concentrated sulfuric and perchloric acids (Fisher Scientific, for Trace Metal Analysis) diluted in ultrapure water (resistivity not less than 18 MΩcm) obtained from an Elgastat water purification system (USF Ltd., Bucks, UK).

4. Results and Discussions

4.1. Results in Perchloric Acid. Figure 2 shows cyclic voltammograms of an Au(111) single-crystal electrode in 0.1 M $HClO_4$ and 0.1 M $KClO_4$ + 1 mM $HClO_4$. The main features of these voltammograms agree well with those previously published for this surface.[26] A set of potential transients, corresponding to the same electrode in 0.1 M $HClO_4$, is shown in Figure 3. The transients are negative in the low potential region. Their magnitude decreases as the electrode potential increases, passing through a negligible value around 0.19 V (SCE), and becoming positive at potentials higher than this value. From the discussion in the Preliminary Considerations section, the potential where the transient is negligible can be identified with the potential of maximum entropy of formation of the double layer.

More information can be extracted by plotting the potential transient as a function of the reciprocal of $\sqrt{t}$, according to eq 5. Such a plot is shown in Figure 4 using the data from Figure 3. A good linear relation is observed for all the potential transients, giving support to the use of eq 4. Apart from a proportionality constant, the slope of the plots of Figure 4 gives a measure of $(\delta E)/(\delta T)_q$ from which, according to eq 6, ΔS can be obtained, by integrating a plot of the slopes as a function of charge. The results are shown in Figure 5. Also in Figure 5 are shown the slopes extracted from similar experiments performed in 0.1 M $KClO_4$ + 1 mM $HClO_4$ solution. We can see that the variation of the slope with the electrode potential is similar for both curves, but the one corresponding to the higher pH is displaced upward. This displacement results in a value of the pzt for this solution ca. 50 mV more negative, than for the lower pH. This vertical displacement can be explain considering the existence of a thermodiffusion potential, as outlined in the section 2.2, which will be higher (more negative) in the more acidic solution, due to the abnormally high transported entropy of the protons (see Table 1). Using values for the entropies of transport of H^+ and ClO_{4-} tabulated in Table 1, a value of ca. -0.38 mV K^{-1} is obtained for $\Delta E_{\text{Thermodiffusion}}/\Delta T$ in 0.1 M $HClO_4$, according to eq 7. Introducing this value into eq 5, using estimated values for ΔT_0 from eq 2 it is possible to show that the obtained slopes should be corrected by adding a constant

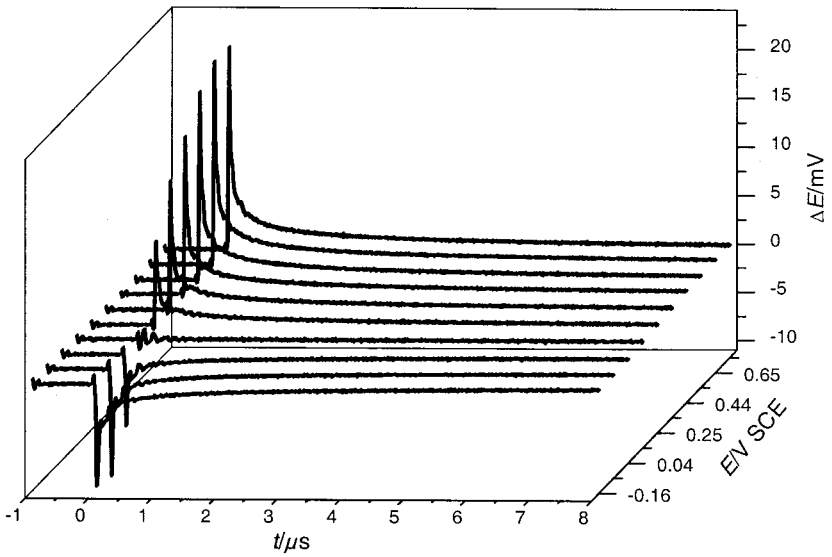

Figure 3. Potential transients after the laser pulse corresponding to a Au(111) electrode in 0.1 M $HClO_4$.

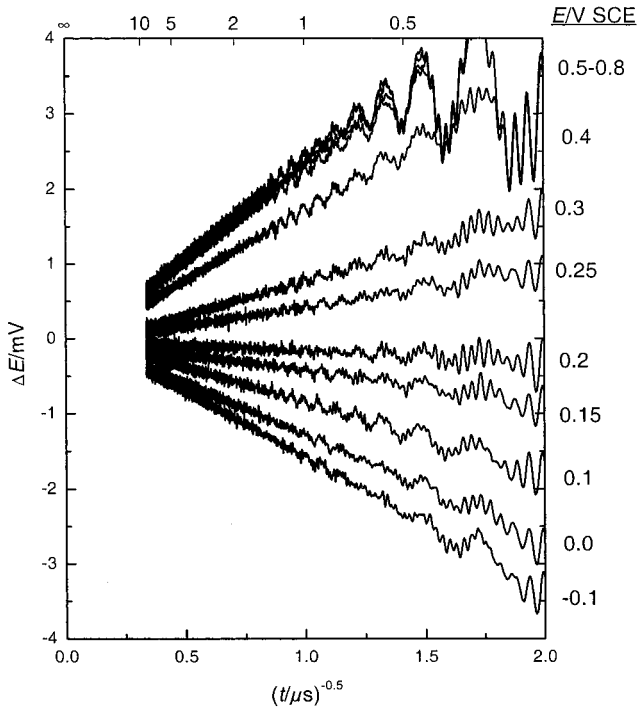

Figure 4. Plot of the potential transients corresponding to a Au(111) electrode in 0.1 M $HClO_4$ as a function of the reciprocal of $\sqrt{t}$.

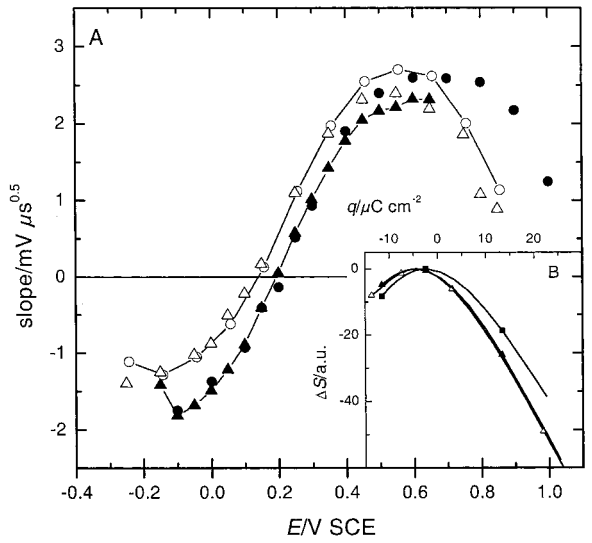

Figure 5. Plot of the slope of the potential transients in Figure 4 as a function of potential for 0.1 M $HClO_4$ (closed symbols) and 0.1 M $KClO_4$ + 1 mM $HClO_4$ (open symbols) solutions. Circles and triangles correspond to different experiments. B) Plot of ΔS as a function of the interfacial charge obtained by integrating the slopes in A as a function of the charge. Squares are uncorrected for the thermodiffusion potential. Open and closed symbols as in A.

displacement of ca. 0.2 mV $\mu s^{0.5}$. Similarly, a value of -0.05 mV K^{-1} is estimated for the 0.1 M $KClO_4$ + 1 mM $HClO_4$. Although this estimation is uncertain since it has been made using transport numbers calculated from ionic conductivities at infinite dilution, it shows that for these conditions the thermodiffusion effect is almost negligible.

By integrating the plot of slopes against charge, a nearly parabolic curve is obtained for ΔS, as shown in Figure 5B with a maximum entropy of formation of the interface at slightly negative charges (ca. -5 μC cm^{-2}). The integration constant has been obtained by arbitrarily setting the maximum entropy to zero. The slopes corresponding to the lower pH have been

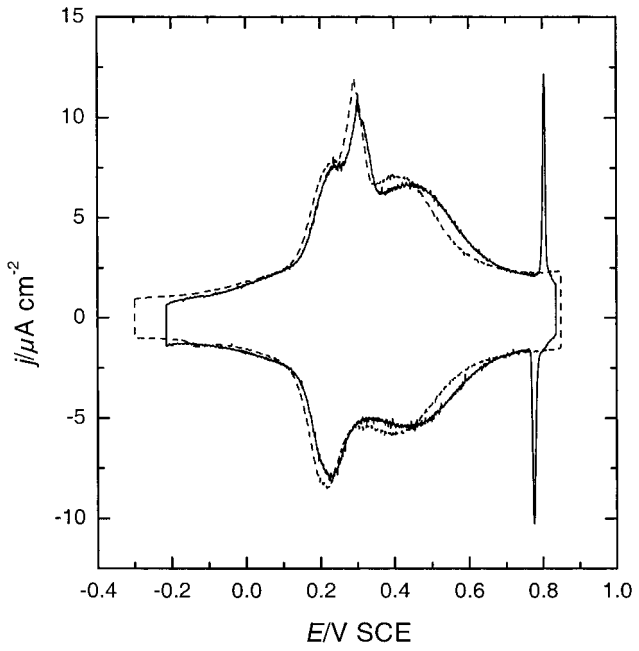

Figure 6. Cyclic voltammograms corresponding to a Au(111) electrode in 0.1 M H_2SO_4 (solid line) and 0.1 M K_2SO_4 + 1 mM H_2SO_4 (dashed line) solutions.

corrected using the thermodiffusion potential calculated above. The result is similar to that obtained with mercury electrodes[4−7] and the location of the maximum has been explained considering that the water molecules are naturally oriented at the pzc, with the oxygen end directed toward the metallic surface. Then, a small amount of negative charge is necessary in order to obtain the situation of maximum degree of looseness of the adsorbed water dipoles that correspond to the potential of maximum entropy.

One point that needs clarification is the existence of electrochemically induced surface reconstructions. The Au(111) surface is well-known to be reconstructed at negative charges, while the reconstruction is lifted at potentials higher than the pzc. Due to the methodology used in the present technique, since the electrode potential is held at each value, the thermodynamic properties obtained would correspond to the surface, either (1 × 1) or reconstructed, that is more stable at each potential.

4.2. Results in Sulfuric Acid. Figure 6 shows a cyclic voltammograms, at 50 mV s^{-1}, corresponding to a Au(111) single-crystal electrode in 0.1 M H_2SO_4 and in 0.1 M K_2SO_4 + 1mM H_2SO_4 solutions. These voltammograms are in accordance to those previously published for this surface.[26] The peak at 0.30 V SCE has been attributed to the lifting of the (px$\sqrt{3}$) reconstruction that takes place at the lower potential region[27] while the two sharp spikes around 0.8 V SCE are explained as due to the formation of an ordered sulfate adlayer. STM experiments have evidenced an ($\sqrt{3}$x$\sqrt{7}$)R19.1° structure at potentials more positive than these spikes.[28] The presence of these spikes in the voltammogram of Figure 6 is a clear indication of the quality of the surface employed for this study.[29] These spikes disappeared when the pH of the solution is increased, in agreement with what has been previously reported.[30]

The potential transients obtained after the laser illumination of the electrode in the 0.1 M H_2SO_4 solution are shown in Figure 7. They exhibit a behavior qualitatively similar to that obtained in perchloric acid solution at potentials between -0.15 and 0.40 V: negative transients at the lower potential region becoming positive at potentials higher than 0.40 V. However, a different

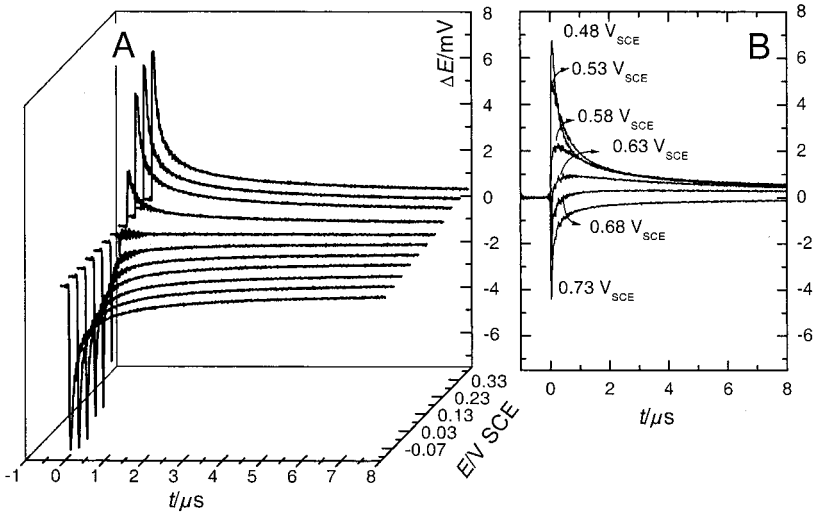

Figure 7. Potential transients after the laser pulse corresponding to a Au(111) electrode in 0.1 M H_2SO_4.

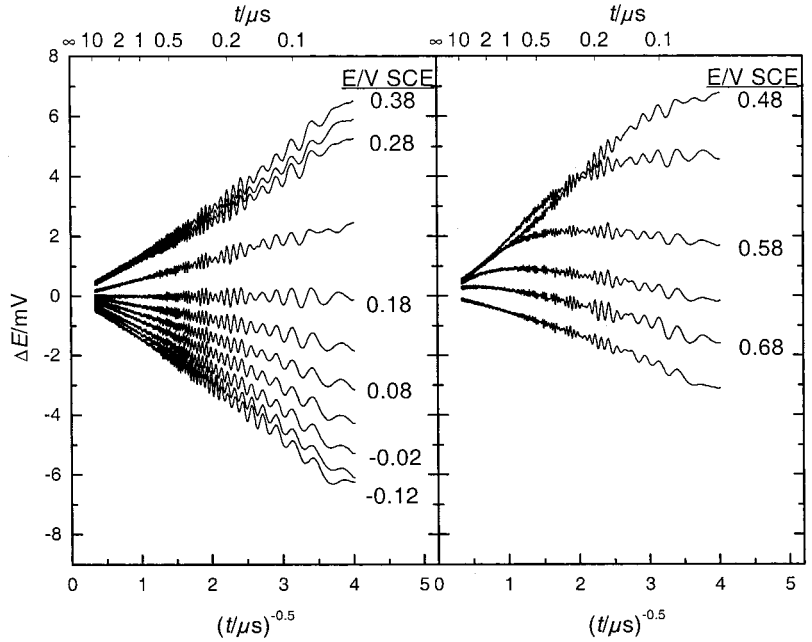

Figure 8. Plot of the potential transients of Figure 7 as a function of $1/\sqrt{t}$.

behavior is observed for potentials higher than 0.70 V. In this potential region the magnitude of the transient decreases as the potential is increased indicating a decrease of the temperature coefficient of the open circuit potential, $(\partial E/\partial T)_q$. At potentials higher than 0.75 V the transient becomes positive. Besides, at potentials between 0.55 and 0.70 V the transient shows a bipolar shape, negative at the beginning, becoming positive at longer times.

Following the same procedure as before, the potential transients have been plotted as a function of the reciprocal of $\sqrt{t}$ in Figure 8. A linear relation is observed for potentials between −0.15 and 0.40 V. However, at potentials higher than 0.4 V the lines become curved. As before, where the linear relation holds, is it possible to calculate a relative measurement of the entropy of formation of the double layer by plotting the slope as a function of the charge and integrating. Although the plot is not linear for potentials higher than 0.40 V, the change in the sign of the transient at potentials higher than 0.75 V implies a decrease in the slope of the decrease of the entropy of formation of the interface when the adsorption of sulfate takes place. Unfortunately, the lack of linear behavior in the plot of Figure 8 at high potential limits the extension of this analysis to this potential region.

Before integrating the slopes of the lines in Figure 8, let us consider first the nature of the 'anomalous' behavior at potentials between 0.4 and 0.75. To explain the shape of the potential transients in this potential region, where adsorption of sulfate takes place, we have to consider that the establishment of the potential drop after the sudden increase of the temperature is not immediate. The bipolar shape of the curves in Figure 7 suggests that there is more than one relaxation time for the establishment of the potential drop. One possible explanation for that is the existence of a thermodiffusion potential. By using the tabulated data in Tables 1 and 2 it is possible to calculate the expected thermodiffusion coefficient, and a value of −0.34 mV K^{-1} is obtained. The sign of this result is in agreement with the observed contribution in the transients of Figure 7 at short times. The curvature of the plot of the potential transients in Figure 8, in this potential region, suggests the necessity to take into account the existence of a finite relaxation time for achieving equilibrium after the alteration of the interfacial

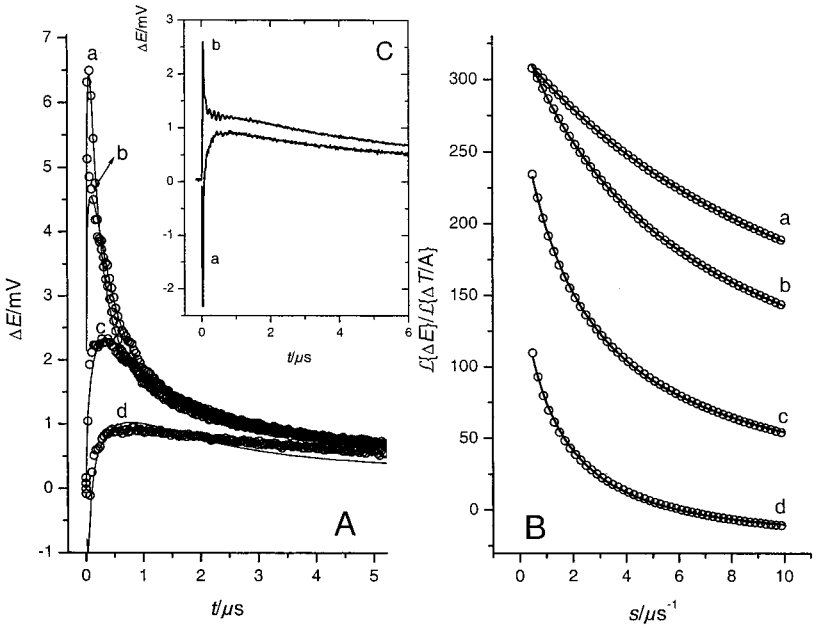

Figure 9. Fit of the potential transients A) in real space; B) in the Laplace space: a) 0.48 V_{SCE}, b) 0.53 V_{SCE}, c) 0.58 V_{SCE}, and d) 0.63 V_{SCE}. C) Comparison of two potential transients obtained in 0.1 M H_2SO_4(a) and 0.1 M K_2SO_4 + 1 mM H_2SO_4 (b) solutions at 0.63 and 0.53 V SCE, respectively.

temperature. According to this hypothesis, equations (10) to (14) should be used to understand the shape of these potential transients.

Figure 9 shows the potential transients in this region, together with their best fit obtained using eq 14. The results are shown both in real space (A) and in Laplace space (B). We should bear in mind that equations (2) and (3) are approximations corresponding to a uniform laser irradiation both in time and in space, and this could justify the small departure between the experimental transients and their fits. With this procedure, the values of ξ_1 can be used to calculate the slope that should be obtained in a plot such as that in Figure 8 if the process would be infinitely fast.

From the shape of the transients in Figure 9A it is clear that there are two contributions to the potential transient with two different time constants. However, the identification of the fast contribution with the thermodiffusion potential is still speculative. More support for this hypothesis can be obtained from the experiments performed in mixtures of 0.1 M K_2SO_4 + 1 mM H_2SO_4. For this solution, a smaller and positive thermodiffusion coefficient (0.045 mV K^{-1}) can be calculated using the data in Tables 1 and 2. Figure 9C shows the comparison between potential transients obtained in 0.1 M H_2SO_4 and in 0.1 M K_2SO_4 + 1 mM H_2SO_4. Clearly, the fast response at short times changes sign when the pH is increased, giving support to its assignment to a thermodiffusion potential.

The slopes extracted from the plot in Figure 8 are plotted as a function of the electrode potential in Figure 10, together with those extracted from the analysis of the Laplace transform of the transients, outlined in the previous paragraph. Also shown in Figure 10 are the slopes extracted from the experiments in 0.1 M K_2SO_4 + 1 mM H_2SO_4. Similarly to what is observed in perchloric/perchlorate solutions, the curves corresponding to the two pHs are displaced vertically, crossing the *x* axis at 0.08 and 0.17 V, for the higher and lower pH, respectively.

Also in Figure 10B are shown the relaxation times, obtained from the fit of the experimental potential transients to eq 14. The positive cycle of the cyclic voltammogram has been plotted in the same figure for the sake of comparison. It is clear than

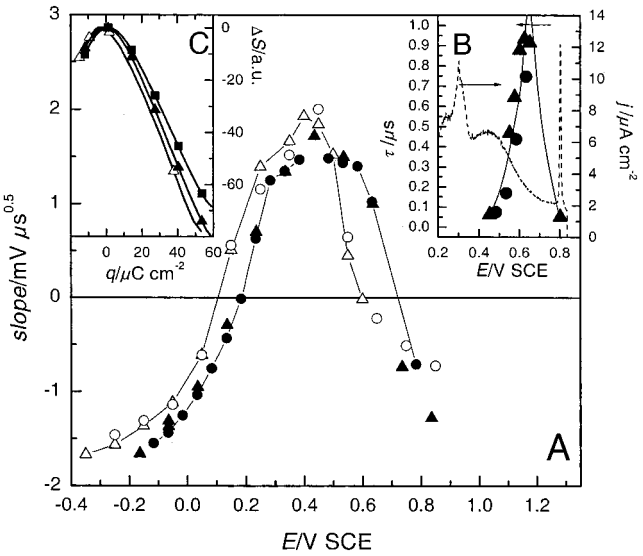

Figure 10. A) Plot of the slope of the potential transients in Figure 8 as a function of potential for in 0.1 M H_2SO_4 (closed symbols) and 0.1 M K_2SO_4 + 1 mM H_2SO_4 (open symbols) solutions. Circles and triangles correspond to different experiments. B) plot of the relaxation time as a function of potential. The positive sweep of the cyclic voltammogram in this potential has been overlapped for the sake of comparison. C) Plot of ΔS as a function of the interfacial charge obtained by integrating the slopes in A as a function of the charge. Squares are uncorrected for the thermodiffusion potential. Open and closed symbols as in A.

the increase of the relaxation time occurs just before the spike corresponding to the disorder/order phase transition. FTIR studies[31] of sulfate adsorption on Au(111) have detected significant spectral changes for the sulfate absorption band in the same potential region, namely, a narrowing and a positive displacement of the band. These features have been interpreted suggesting that sulfate anions start to form short-range domains in this potential region. This process would be coupled with the breaking of the ice-like structure of water molecules believed to be present at lower potentials and the forming of water-sulfate hydrogen bonds.[31] Short-range associations of sulfate molecules

have also been suggested to explain STM observations of granular features in the same potential region.[30] The existence of bidimensional sulfate islands of lower mobility, growing in this potential region, seems a reasonable explanation for the increase of the relaxation time observed in the present work.

Finally, Figure 10C shows the entropy change of formation of the double layer obtained, as before, integrating the slopes of the transients in Figure 10A. The curve corresponding to 0.1 M H_2SO_4 has been obtained after correcting the slopes with a tentative value of the temperature coefficient of the thermodiffusion potential, calculated with eq 7. The uncorrected curve has been also included for comparison. As before, the integration constant has been obtained by arbitrarily setting the maximum entropy to zero. As observed in the perchloric acid solution, the potential of maximum entropy is located at potentials slightly negative to the pzc.

5. Conclusions

We have shown that illumination of an Au(111) single-crystal electrode surface with short pulses of high-power laser light can be used to suddenly increases its temperature. From the evolution of the open circuit potential during the temperature relaxation it has been possible to obtain a relative measurement of the entropy of formation of the double layer. Although absolute values of this magnitude would need an independent calibration of the temperature change, the relative variations of the entropy of formation of the double layer can be obtained without this calibration. In particular, a key result easily obtained from this methodology is the electrode potential where the potential transient is zero (pzt), which can be identified with the potential of maximum entropy of formation of the double layer. The pzt is located at a potential slightly negative to the potential of zero charge in the two solutions studied. This result is expected from the models of the double layer. According to these models, at the pzt there is a maximum looseness of the adsorbed water dipoles, with a negligible contribution to the potential drop. On the other hand, the observation of a positive temperature coefficient at the pzc implies a net negative contribution of the adsorbed water layer at this potential, which imply a net orientation of the water molecules with the negative end directed toward the surface.

Another interesting observation has been done in the case of sulfuric acid solutions, where a sharp increase of the relaxation time after the temperature change has been observed at potentials just below the phase transition to form the ($\sqrt{3}$x$\sqrt{7}$) adlayer. This has been explained in terms of formation of sulfate islands of reduced mobility in this potential region.

Acknowledgment. V.C gratefully acknowledges the European Commission for the award of a Marie Curie Fellowship under the European Community program "Improving Human Research Potential and the Socio-economic Knowledge Base" under contract number HPMFCT-2000-00529. The PTCL electronic workshop is gratefully acknowledged for the development of the potentiostat used in this work. We thank Prof. J. Feliu for providing the Au(111) single crystal.

References and Notes

(1) Clavilier, J. *J. Electroanal. Chem.* **1980**, *107*, 211−216.
(2) Clavilier, J.; Faure, R.; Guinet, G.; Durand, R. *J. Electroanal. Chem.* **1980**, *107*, 205−209.
(3) Clavilier, J. Flame-Annealing and Cleaning Technique. In *Interfacial Electrochemistry*; Wieckowski, A., Ed.; Marcel Dekker: New York, 1999; pp 231−248.
(4) Hills, G. J.; Hsieh, S. *J. Electroanal. Chem.* **1975**, *58*, 289−98.
(5) Harrison, J. A.; Randles, J. E. B.; Schiffrin, D. J. *J. Electroanal. Chem.* **1973**, *48*, 359−381.
(6) Hills, G. J.; Payne, R. *Trans. Faraday Soc.* **1965**, *61*, 326−349.
(7) Silva, A. F. In *Trends in Interfacial Electrochemistry. ACS symposium series*; Silva, A. F., Ed.; D. Reidel Publishing Company, 1986; pp 49−70.
(8) Silva, F.; Sottomayor, M. J.; Martins, A. *J. Chem. Soc., Faraday Trans.* **1996**, *92*, 3693−3699.
(9) Silva, F.; Sottomayor, M. J.; Martins, A. *J. Electroanal. Chem.* **1993**, *360*, 199−210.
(10) Silva, F.; Sottomayor, M. J.; Hamelin, A.; Stoicoviciu, L. *J. Electroanal. Chem.* **1990**, *295*, 301−316.
(11) Silva, F.; Sottomayor, M. J.; Hamelin, A. *J. Electroanal. Chem.* **1990**, *294*, 239−251.
(12) Hamelin, A.; Stoicoviciu, L.; Silva, F. *J. Electroanal. Chem.* **1987**, *229*, 107−124.
(13) Hamelin, A.; Stoicoviciu, L.; Silva, F. *J. Electroanal. Chem.* **1987**, *236*, 283−294.
(14) Benderskii, V. A.; Velichko, G. I. *J. Electroanal. Chem.* **1982**, *140*, 1−22.
(15) Benderskii, V. A.; Velichko, G. I.; Kreitus, I. *J. Electroanal. Chem.* **1984**, *181*, 1−20.
(16) Smalley, J. F.; Chalfant, K.; Feldberg, S. W.; Nahir, T. M.; Bowden, E. F. *J. Phys. Chem. B* **1999**, *103*, 1676−1685.
(17) Smalley, J. F.; Geng, L.; Feldberg, S. W.; Rogers, L. C.; Leddy, J. *J. Electroanal. Chem.* **1993**, *356*, 181−200.
(18) Smalley, J. F.; Krishnan, C. V.; Goldman, M.; Feldberg, S. W.; Ruzic, I. *J. Electroanal. Chem.* **1988**, *248*, 255−282.
(19) Climent, V.; Coles, B. A.; Compton, R. G. *J. Phys. Chem. B* **2001**, *105*, 10669−10673.
(20) Schulz, L. G. *J. Opt. Soc. Am.* **1954**, *44*, 357−362.
(21) Von Allmen, M.; Blatter, A. *Laser-beam interactions with materials: physical principles and applications*, 2nd updated/ed.; Springer: Berlin; London, 1995.
(22) Agar, J. N. In *Adv. Electrochem. Electrochem. Eng.*; Delahay, P., Tobias, C. W., Eds.; Wiley-Interscience: New York, 1963; Vol. 3; pp 31−121.
(23) Smalley, J. F.; MacFarquhar; Feldberg, S. W. *J. Electroanal. Chem.* **1988**, *256*, 21−32.
(24) Smalley, J. F.; Krishnan, C. V.; Goldman, M.; Feldberg, S. W.; Ruzic, I. *J. Electroanal. Chem.* **1988**, *248*, 255−82.
(25) Clavilier, J.; Armand, D.; Sun, S.-G.; Petit, M. *J. Electroanal. Chem.* **1986**, *205*, 267−277.
(26) Hamelin, A. *J. Electroanal. Chem.* **1996**, *407*, 1−11.
(27) Kolb, D. M. *Prog. Surf. Sci.* **1996**, *51*, 109−173.
(28) Edens, G. J.; Gao, X.; Weaver, M. J. *J. Electroanal. Chem.* **1994**, *375*, 357−366.
(29) Dretschkow, T.; Wandlowski, T. *Ber. Bunsen-Ges. Phys. Chem.* **1997**, *101*, 749−757.
(30) Cuesta, A.; Kleinert, M.; Kolb, D. M. *Phys. Chem. Chem. Phys.* **2000**, *2*, 5684−5690.
(31) Ataka, K. I.; Osawa, M. *Langmuir* **1998**, *14*, 951−959.
(32) Breck, W.; Cadenhead, G.; Hammerli, M. *Trans. Faraday Soc.* **1965**, *61*, 37−49.